

BACHELORARBEIT

STATISTICAL VALIDATION AND VISUALIZATION OF CAUSAL INFERENCE WITH EXTREMES IN WIND-TURBINE DATA SET

Verfasserin ODER Verfasser

Kejsi Hoxhallari

angestrebter akademischer Grad

Bachelor of Science (BSc)

Wien, 2023

Studienkennzahl lt. Studienblatt: A 033 521

Fachrichtung: Informatik - Data Science

Betreuerin / Betreuer: RNDr. CSc.Katerina Schindlerova

Contents

1	Introduction	4
1.1	Dataset	5
1.2	Heterogeneous Graphical Granger Causality by Minimum Message Length	5
2	Related Work	6
2.1	Granger Causality for Causal Inference	7
2.1.1	Definition	7
2.1.2	Granger Causality in Climatology, its Drawbacks and Advantages	7
3	Main Idea	10
3.1	Scenarios and Selection of Their Time Intervals	10
3.2	Best Fitting Exponential Distribution	11
3.3	Finding Lag Length	12
3.4	Method HMML	13
3.4.1	Granger Causal Model	13
3.4.2	The Heterogeneous Graphical Granger Model	13
3.4.3	Minimum Message Length	14
4	Implementation	15
4.1	Identifying Instances of Extreme/Moderate Wind	15
4.2	Code for HMML	15
4.3	Experiments with HMML	16
4.4	Statistical validation	16
4.5	Visualization	17
5	Results and Discussion	19
5.1	Scenario 1: Winter Half-Year, High Wind Speed Modality	19
5.2	Scenario 2: Summer Half-Year, High Wind Speed Modality	19
5.3	Scenario 3: Winter Half-Year, Low Wind Speed Modality	19
5.4	Scenario 4: Summer Half-Year, Low Wind Speed Modality	20
5.5	Scenario 5: Winter Half-Year, Moderate Wind Speed Modality	20
5.6	Scenario 6: Summer Half-Year, Moderate Wind Speed Modality	20
5.7	Beta values	33
6	Conclusions	40
7	Future Work	41

Abstract

In this work we investigate 10 meteorological variables measured in the wind farm in Andau, Austria, and their causal effect on wind speed for each of the 38 wind turbines. These variables were selected as the most relevant variables for wind speed and are given in the form of time series of hourly measurements over time period 2000-2020. Knowing the probability distribution of wind speed in a concrete time interval, we employ the causal inference method HMML. HMML is a multivariate Granger causal model for time series from exponential family and its causal inference is done by the minimum message length. We statistically validate the results for various scenarios (low extreme wind, moderate wind speed and high extreme wind in a concrete hydrological half-year) and provide visual outputs in the form of pie charts to display the causal strength of each variable on wind speed for every turbine and every wind speed scenario. We believe that these visual outputs could contribute to the knowledge discovery or to the decision strategies for the experts in climatology or the wind power companies.

1 Introduction

As energy demand rises, environmental pollution and efforts to mitigate climate change become key drivers of significant growth in renewable energy, including wind energy and thus the importance of the development of large wind farms increases [25]. However, the management of wind turbine farms is strongly dependent on the behavior of the wind [13]. For the turbines to be fully utilized, meteorologists need to have precise mathematical models that characterize these processes. Even more importantly, due to the fast variability of wind, models of wind forecasting are crucial and sometimes even legally required [8] for wind power prediction in wind farms.

Appropriate meteorological parameters and data that may indicate future trends should be considered in the prediction of wind power generation [10] in order to obtain more reliable and accurate results. In this work we focus on the question, how other wind-related variables such as pressure, density, etc. influence periods of strong, low, and moderate wind. The goal is to gain a better understanding of the conditions that lead to extreme wind events. The obtained knowledge would be then be used as an indicator to turn off the wind turbines or keep the turbines running when there are "calm" periods.

Additionally, wind-related atmospheric parameters have been shown to be significant in predicting wind turbine energy production, which in turn is essential to the evaluation of the economic profit of the farms [4]. As a result, it is critical to assess temporal relationships between various wind-related meteorological variables. In this work we use word "causal" while meaning Granger-causal.

We focus on four main research questions:

RQ1 - Identifying the extreme events and calm periods of wind for the last 20 years in the Andau wind farm

RQ2 - How strong (if any) is the causal relation of each of the meteorological variables to wind speed in the farm in a concrete climatological scenario?

RQ3 - Which meteorological variables are causal in these scenarios, and what are the differences among the causal variables in these scenarios?

RQ4 - Create a visualization for the individual influence of the variables on each of the 38 turbines

1.1 Dataset

We considered the data set from Geosphere Austria of the wind farm located in Andau, Eastern Austria, which consists of 24 spatial and weather variables related to 38 individual wind turbines over the span of 20 years (2000-2020) measured hourly. However, only 10 of these variables are taken into account for the results and we discuss the selection of these variable in Section 3.

Figure 1 shows the topography of the 38 turbines at the Andau farm.

1.2 Heterogeneous Graphical Granger Causality by Minimum Message Length

The method used to analyze the data and calculate the impact of each of the 10 weather parameters is the Heterogeneous Graphical Granger Causality by Minimum Message Length (HMML) [16]. HMML is used for causal inference among processes with distributions from an exponential family, and as an optimization criterion it uses the minimum message length principle to overcome overestimation that might happen in shorter time series if we use the heterogeneous graphical Granger model. By short time series are meant time series with the length n , where n is of magnitude of at most of thousands with respect to the number of time series p .

The idea of minimum message length, introduced by Wallace and Dowe in [29] follows this concept: It selects the model that produces the most concise explanation of data as more likely to be correct even in cases where alternative models have the same fit-accuracy measurements.

Given that the heterogeneous graphical Granger causality by minimum message length has been shown to be very efficient on short time series, it makes sense to use it in climatic processes that are dynamic and thus measured on relatively short time intervals, such as those in our case. For our experiments with the data of the

Andau wind farm and based on the expert knowledge from GeoSphere Austria, we select time intervals of 96 hours in two independent hydrological half-years for each year to observe and assess the influence of wind variables in these half-years, respectively, and in relation to wind speed. The lengths of the two hydrological half-years that we use in the experiments are defined according to this definition [2] and are as follows: The winter hydrological half-year runs from November 1st to April 31st, and the summer hydrological half-year runs from May 1st to October 31st.

2 Related Work

Here we shortly report about related work on investigating temporal relationships and forecasting related to climatological processes. Approaching these tasks, various statistical methods were used in the literature.

Colquhoun and Riley use in [11] simple multiple regression analysis to determine the relationships between tornado intensity and other wind-related parameters such as wind speed, vertical wind shear, colder temperatures, streamwise vorticity, storm velocity, and so on. Later publications have used fuzzy logic and artificial neural networks (ANN) to forecast wind speed, such as the seminal work from Monfared al. [22], which first demonstrated that these methods outperform traditional fuzzy predictors in terms of accuracy and speed. Another publication [17] uses deep neural networks (DNN) to forecast wind power for offshore wind turbines by investigating correlation coefficients. This approach also produced high accuracy results. Zi Lin al. also applied feature dimension reductions by evaluating less significant features which also spared more computation cost. A considerable amount of literature has been using artificial neural networks and support vector machines (SVM) for the prediction within the wind variables in wind farms [24] [9] [26] among others. Autoregressive integrated moving average (ARIMA) method has also been prominent in literature due to its robustness [7] especially in combination with other methods such as ANN, particularly important and effective in short time series of 24-48 h in wind speed prediction.

Most of the cited studies, however, concentrate on detecting correlations rather than pinpointing the most influential parameters, which we are trying to achieve in our study.

2.1 Granger Causality for Causal Inference

2.1.1 Definition

Granger causality can be explained as a temporal relationship that is based on prediction and where the cause occurs before the effect and it is used under the presumption that cause helps predict the effect [15]. Multivariate Granger causality is used when the number of time series p is more than or equal to 2. For a more detailed definition we refer to Section 3.4 of this work and the paper by Kateřina Hlaváčková-Schindler al. [16] Section 2.1.

2.1.2 Granger Causality in Climatology, its Drawbacks and Advantages

One study [28] combines forecasting and causal inference approaches to predict influential weather variables such as solar wind on space weather using an information theory framework, concluding that using both approaches yields the best results in predicting influence. It is argued in the paper that the reason we obtain better results is because, according to Granger causality principles, forecasting is associated with the identification of causal variables responsible for state transitions. When it comes to investigating cause-effect relationships, the usage of time-series methods based on the notion of multivariate Granger causality has gained popularity [12]. The Granger causality notion has been well adopted in many fields, especially in healthcare and climatology. In the paper by Goebel et al. [14] a framework is presented in the context of multivariate Granger causality to determine the most influential brain areas using time-resolved fMRI data. In wind forecasting, the Granger causality test was used as a technique to select important input for the proposed hybrid model [18].

Despite of the popularity of Granger causality, there is an ongoing discussion concerning Granger causality’s relevance for causal inference, [21] that says Granger causality might be unsuitable when the researcher doesn’t have prior knowledge of the phenomenon being studied. In our study case, it is relevant since we have prior knowledge of which variables are more likely to be related, hence the selection of only 10 out of the initial 24 variables in the data set. Another argument in favor of using Granger causality methods can be based on the recent Nature publication [20]. According to

that paper, if the theoretical background of investigated processes is insufficient, graphical Granger models are helpful for inferring causal relations from data. These methods can also make possible to perform credible analyses with a large amount of observational time data, e.g. in brain networks [19], since they are much less costly than e.g. common epidemiological research.

However, Granger causality poses another challenge: It can be inapplicable to non-Gaussian distributions. Since weather data are known to be processes that have different data distributions, we must look at methods that are suitable for non-Gaussian distributions. There have been some efforts to overcome such difficulties, such as in this study [3] where a modified version of the Granger graphical model by adding Penalized Vector Autoregression (VAR) has been used to discover temporal dependencies in time-series that are considered "irregular." Another publication [27] also uses lasso penalty on Granger causality concept for biological systems. For dealing with data having generally non-Gaussian distributions Behzadi et al. [5] introduced the Heterogeneous Graphical Granger Model (HGGM). HGGM utilizes regression in generalized linear models (GLM) with adaptive lasso penalization. This makes HGGM suitable for a broader class of distributions from the exponential family. For our experiments, we are using heterogeneous graphical Granger causality by minimum message length, which uses the HGGM model from [5] but expands it for the use case of short time series, when the number of time series is of the order at most 1000 greater than the number of observations.

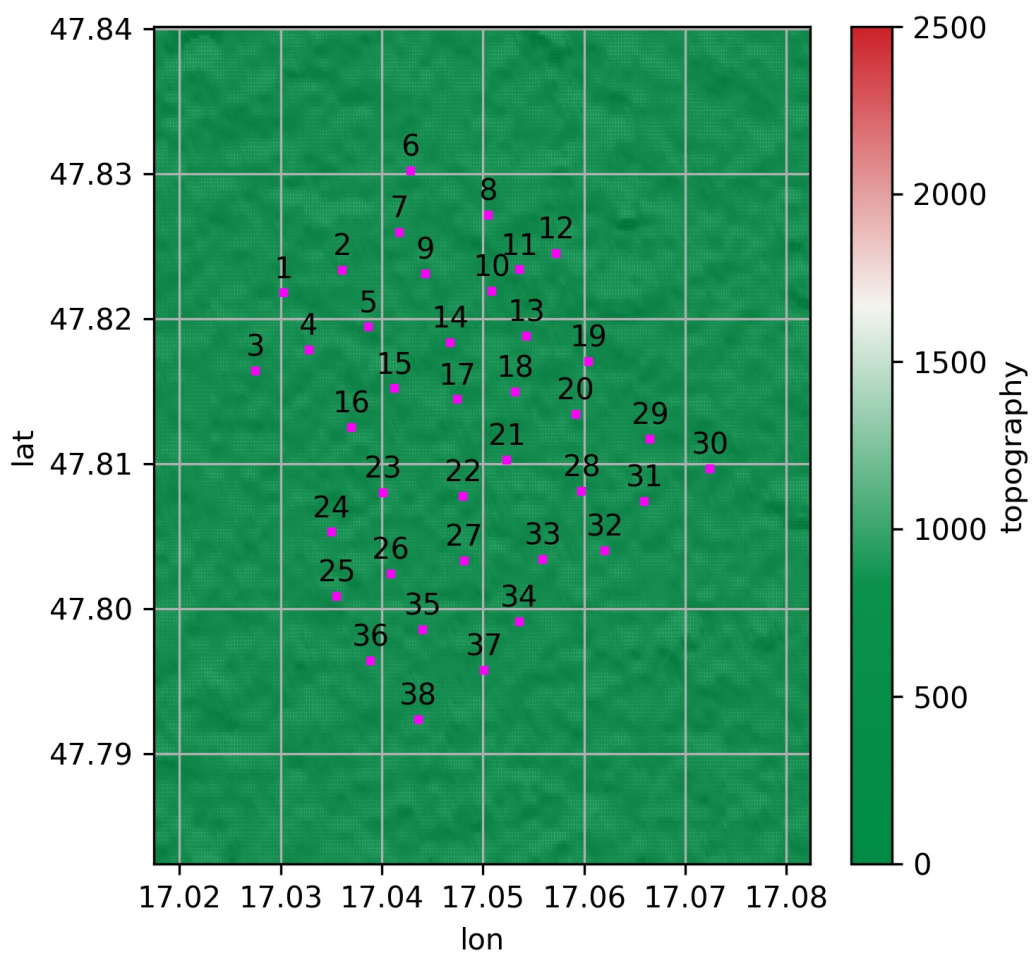


Figure 1: Wind turbines in Andau, Eastern Austria, © I. Schicker, Geosphere Austria

3 Main Idea

Utilizing the ERA-5 data we investigate 10 wind-related meteorological variables identifiable according to the database of climatological temporal measurements in Europe [1] as described in the Table 1 below.

Abbreviation	Description	Unit
bhl	Boundary Layer height	m
d2m	Divergence at 2 m	s^{-1}
z	Geopotential	$m^2 s^{-2}$
r	Relative Humidity	%
t2m	Temperature at 2 m	K
t100m	Temperature at 100 m	K
t135m	Temperature at 135 m	K
wdir100m	Wind direction at 100 m	degree radians
wspeed135m	Wind speed at 135m	ms^{-1}
wspeed100m	Wind speed at 100 m	ms^{-1}

Table 1: Meteorological variables considered

We want to discover which of these variables have a causal effect on wind speed at 135m, which is the position of each turbine in extreme wind scenarios and in calm periods. Based on the knowledge of the scientists from Geosphere Austria, as extreme events we consider a wind speed of $\geq 15 m/s$ where $15 m/s$ is the maximum value of wind speed before the wind turbines must be turned off as well as a wind speed of $\leq 2 m/s$ as minimum value of wind speed. As moderate wind we consider wind with speed: $6 m/s \leq ws \leq 8 m/s$.

3.1 Scenarios and Selection of Their Time Intervals

For the preprocessing of the data we first search for all of the occurrences of low/high wind or wind that falls within the 'moderate' category as denoted above. Then several suitable time intervals of 96 hours are selected for the three scenarios in all years, separately for the summer half-year and the winter half-year as illustrated in Table

2. The goal is to have at least 10% instances of extreme/moderate wind in each of the intervals.

Scenarios		
Wind speed modality	Winter half-year	Summer half-year
High Wind	2000-01-16 - 2000-01-19	2000-10-28 - 2000-10-31
Low Wind	2000-01-01 - 2000-01-04	2000-07-22 - 2000-07-25
Moderate Wind	2000-12-02 - 2000-12-06	2000-06-16 - 2000-06-20

Table 2: Time Intervals considered for year 2000

All of the selected intervals fulfill the condition on short time series.

3.2 Best Fitting Exponential Distribution

To be able to apply HHM method, the distribution function of wind speed in each of the intervals is then evaluated. The best fitting distribution is found by computing the residual sum of squares (RSS) and hypothesis test.

$$RSS = \sum_{i=1}^n (y_i - f(x_i))^2 \quad (1)$$

The set of exponential distributions that is tested is Gaussian distribution, inverse Gaussian distribution and the gamma distribution. Different scenarios may produce different best fitting distributions due to the heterogeneous nature of wind speed, an example is illustrated in Figure 2 below where wind speed function with regards to time is shown for the year 2007.

As can be seen the behaviour of wind varies for scenarios of low, high and medium speed but also from whether it is in the winter or summer season. For the extreme scenarios the wind speed in this case

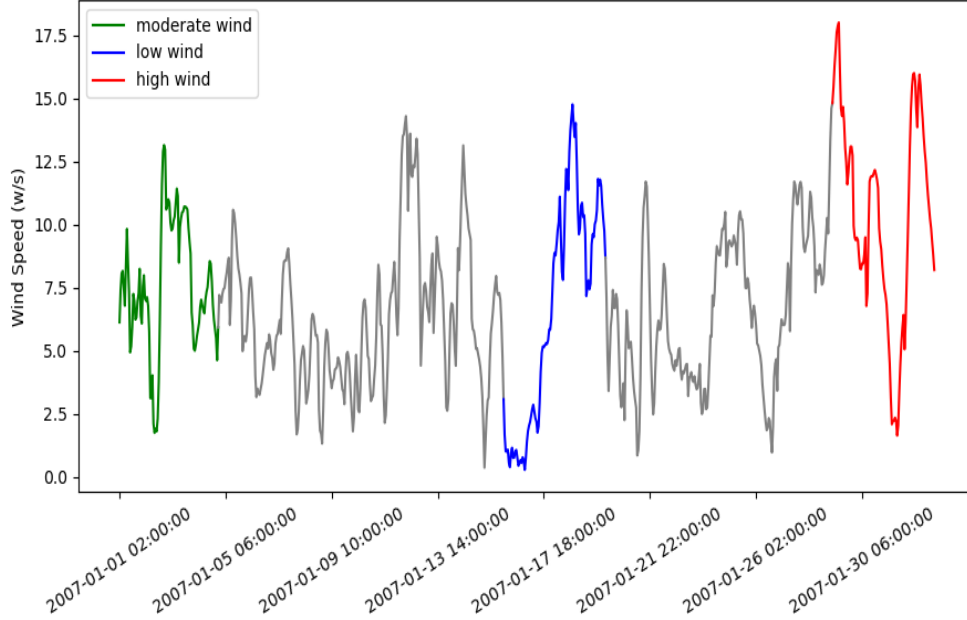


Figure 2: Wind speed with respect to time, year 2007

has a Gaussian distribution whereas for the moderate wind scenario wind speed has a gamma distribution.

The intervals that we have chosen for the three scenarios with different wind speed modalities do not only contain entries of extreme wind but also for example in the high wind interval we have instances of very low wind. This is expected as wind speed is not linear and our aim is to have at least 10% of the interval containing extremes that we are investigating.

3.3 Finding Lag Length

To apply the method for investigating causal influence between the variables we need to be able to first determine the autoregressive lag length of the time series selected. Establishing the right lag length is a significant important step in the evaluation of multivariate time series models [6]. Akaike's information criterion (AIC) is a selection criteria for lag, that has been proven in [23] to be accurate in particular concerning under estimation and short time series.

AIC is defined as followed.

$$AIC = 2k - 2l \quad (2)$$

where l is the log likelihood, k is the number of parameters and n number of samples used for fitting.

The idea of selecting the lag by AIC is to create a number of AR models with different lags d , and with the AIC criteria we can choose the one that fits the best by simply selecting the one lag for which AR(d) gives the minimal AIC value.

3.4 Method HMML

We use the Graphical Granger causal HMML for target variable wind speed. Before going into details how we use the HMML method in our code, some preliminaries about Granger causal model in Section 3.4.1 and the heterogeneous graphical Granger model in Section 3.4.2 are presented. The idea of the minimum message length principle is explained in Section 3.4.3.

3.4.1 Granger Causal Model

Granger causal model extends the autoregressive Granger causality for time series ($p \geq 2$)

$$x_i^t = X_{t,d}^{Lag} \beta_i' + \epsilon_i^t \quad (3)$$

where $X_{t,d}^{Lag} = (x_1^{t-d}, \dots, x_1^{t-1}, \dots, x_p^{t-d}, \dots, x_p^{t-1})$ and β_i be a matrix of the regression coefficients and ϵ_i^t be white noise.

One says that time series x_j Granger causes time series x_i if and only if at least one of the coefficients in the j -th row of β_i is non zero.

3.4.2 The Heterogeneous Graphical Granger Model

The following equations are adopted from paper [16]. The heterogeneous graphical Granger model considers time series x_i where

their probability function is of the exponential type family. The generic density for x_i is:

$$p(x_i|X_{t,d}^{Lag}, \theta_i) = h(x_i) \exp(x_i \theta_i - \eta_i(\theta_i)) \quad (4)$$

where

$$\theta_i = X_{t,d}^{Lag} \cdot (\beta_i^*)' \quad (5)$$

(β_i^* denotes its optimum).

HGGM applies the idea of generalized linear models (GLM) to time series x_i :

$$x_i^t \approx \mu_i^t = \eta_i^t(X_{t,d}^{Lag} \beta_i') = \eta_i^t\left(\sum_{j=1}^p \sum_{l=1}^d x_j^{t-l} \beta_j^l\right) \quad (6)$$

Causal inference in the equation above 6 can be solved with:

$$\hat{\beta}_i = \underset{\beta_i}{\operatorname{argmin}} \sum_{t=d+1}^n (-x_i^t(X_{t,d}^{Lag} \beta_i') + \eta_i^t(X_{t,d}^{Lag} \beta_i')) + \lambda_i R(\beta_i) \quad (7)$$

For given lag $d > 0$, $\lambda_i > 0$, and $t=d+1, \dots, n$ and where $R(\beta_i)$ is the adaptive lasso penalty function.

3.4.3 Minimum Message Length

The minimization of (7) with respect to β values is done by using the MML principle. The minimum message length principle chooses the model that has the shortest message length as the best explanatory for the data. The message is a statement of the model together with data encoded using that model. To decompress this data representation, the specifics of the statistical model used to encode the data must also be included in the compressed data string. Since the problem of finding the minimal message length is a NP problem, HMML uses the Wallace–Freeman approximation [30].

We will not present the equations and criterion for computing the causal values explicitly, for it we refer to Section 3.1 of [16]. We use this criterion only for one i , i.e. only for target variable wind speed.

4 Implementation

For the implementation, Python was used as a programming language. And the code was divided into classes and methods described below.

4.1 Identifying Instances of Extreme/Moderate Wind

We used the dataset introduced in the previous sections to investigate how many extremes there were in each of the years and locate them. The class `Extremes` takes as a parameter: the `data`, the `variable` (in our case, wind speed), the `maximum_value`, `minimum_value` and `moderate_value`. The maximum, minimum, and moderate values will be set to the values defined in Section 3.

The class has three methods: `calculate_lows()`, `calculate_highs()` and `calculate_moderate()` which give as a return value all instances of high/lows/moderate wind instances in the data from that year. The class also contains the method `for_turbine(nr_of_turbine)` in which you can specify the turbine in which you want to find the extremes, not that of the whole farm. The method `loc_extreme()` takes as a parameter the rows of the data which are extremes and outputs only the date of each of them. The method `loc_extreme()` and `calculate_lows()`, `calculate_highs()`, `calculate_moderate()` are used when we try to select each interval for each of the scenarios, to see which interval contains the most extremes and thus can be taken as a suitable representative of each scenario.

4.2 Code for HMML

The python code for the HMML method was provided by Andreas Fuchs, who reimplemented the original version of HMML in Matlab of Kateřina Hlaváčková-Schindler under <https://t1p.de/26f3>. The implementation can be found at <https://git01lab.cs.univie.ac.at/a1106307/hmml>. In our code, we use the HMML method with genetic search algorithm `HMMLGA`.

4.3 Experiments with HMML

After selecting time frames for each scenario/each year, we use the `HMMLParameters` class to calculate the parameters that we need to run the HMML method. It takes as input the start and end of the selected interval and the data. The class has a method called `determine_distribution()` which calculates the distribution of the variable wind speed for a given interval using RSS, and a method `select_lag()` which selects the smallest lag value after fitting the ARIMA model. We use the class `Scenarios` with the method `populate()` to populate the dictionary that holds the data for each of the scenarios. A scenario contains: turbine number, year, season name (one of the six possibilities mentioned in Section 3) :

- Winter half-year, high wind
- Summer half-year, high wind
- Winter half-year, low wind
- Summer half-year, low wind
- Winter half-year, moderate wind
- Summer half-year, moderate wind

scenario begin, scenario end, distribution, lag, and beta values.

Method HMML is run for all of the scenarios to compute their beta values. The method HMML outputs a list of lists with beta values. The number of lists corresponds to the number of variables we are considering to find causality; in our case, that would be 10 variables. Each of the lists contains d entries, d corresponds to the lag value we have determined for each scenario.

4.4 Statistical validation

After the β values for each scenario are found, we run the method `aggregate_betas` which calculates the newly introduced variable beta proportionality in each of the lists containing d values. The beta proportionality of variable i can be understood as the relative strength of causality with respect to all variables. It is calculated as shown in the Equation 8 below.

$$beta_proportionality_i = beta_max_i / sum(beta_max) \quad (8)$$

where β_{max-i} is the maximum value out of d β_i values for variable i . After calculating the beta proportionality, we get one beta value for each variable. For all of the scenarios, we then calculate the corresponding arithmetical mean over all years.

The average was calculated over 20 experiments for each scenario and for each turbine. The total number of experiments is 4560.

4.5 Visualization

For the visualization, we have created 38 interactive pie charts for each season using matplotlib pie charts. The end output is six figures corresponding to the seasons, each of which contains 38 pie charts corresponding to the turbines in the farm. The beta values of the turbine are plotted in the pie chart. First a pie chart is created containing the biggest value of the beta values in the list, then this pie chart is plotted on the grid in the figure. As an interactive feature, when a computer mouse enters the pie chart, the function `hover(event)` is triggered which shows a detailed pie chart with all the rest of its respective beta values. When the mouse leaves the event, the function `leavePie(event)` is triggered, which sets the pie chart back to its original form. All figures contain: a title which is the season and wind modality, a title for which of the plots that is the number of turbine, when mouse enters the pie the strength of causality of each variable is shown in a specific color to discriminate against other variables and with a size of chunk which corresponds to its beta value. Each of the pies is accompanied by a legend showing the concrete beta values, but have been omitted in the figures shown in Section 5 due to consistency reasons.

An example of how the pie chart when mouse enters with the legend looks is shown below in Figure 3. The size of each pie piece shows the relative value of beta for the corresponding variable.

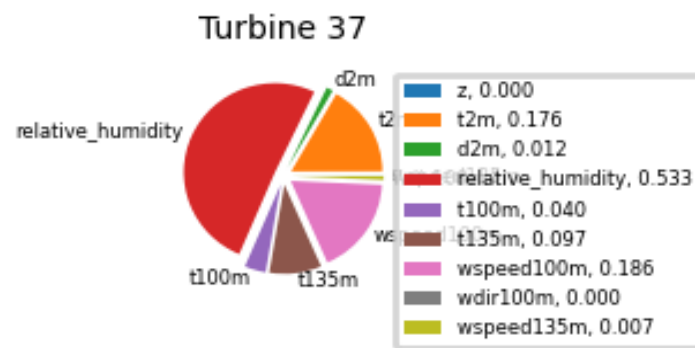


Figure 3: Example of interactive pie chart

5 Results and Discussion

The resulting beta values are plotted for each of the six seasons and each of the 38 turbines. Before clicking on the pie chart, the variable with the strongest causal inference on wind speed is shown. When clicking on each of the pie charts, a more detailed view is shown, illustrating how strongly each of the 10 variables considered influence wind speed in that scenario and measured by that turbine. The figures below illustrate the visualization of the beta values.

5.1 Scenario 1: Winter Half-Year, High Wind Speed Modality

In the winter half-year when there is high wind, as shown by Figure 4 most of the turbines reveal **relative humidity** as the most influential variable on wind speed; however, however **wind speed** is also recognized as the variable with the strongest causality by quite a few turbines, specifically by 12 of them. When we take a deeper look at Figure 5 which shows the details of of the turbines in relation to all other causal variables, we can see that **geopotential (z)** and **temperature** are also relevant variables, as can be seen from the size of the chunk that they determine in each turbine.

5.2 Scenario 2: Summer Half-Year, High Wind Speed Modality

In the second scenario (Figure 6) we can see from the results that **wind speed** is the most influential, as it is the variable that is shown with the biggest beta value from 35 turbines, while the other 3 show **relative humidity**. Looking at Figure 7 we can see that all turbines show similar influences from all variables. The variables that have little causal effect on wind speed are boundary layer height(blh) and wind direction (wdir100m).

5.3 Scenario 3: Winter Half-Year, Low Wind Speed Modality

For the winter half year when investigating low wind modes, Figure 8 shows that all 38 turbines give **relative humidity** as the variable with the biggest beta value. When we see the details of the farm in scenario 3 (Figure 9) we can see clearly that relative humidity

does have a considerably large causal effect (almost 50%) in all of the turbines.

5.4 Scenario 4: Summer Half-Year, Low Wind Speed Modality

For the low wind speed modality in the summer half-year, we have similar results as for the winter half-year: the most dominant variable across all turbines is **relative humidity** but 7 turbines show **geopotential (z)** as the most dominant variable. In this scenario when observing the causal effect of all variables Figure 11 it can be seen that the variables with the lower influence are again boundary layer height(blh) and wind direction(wdir100m).

5.5 Scenario 5: Winter Half-Year, Moderate Wind Speed Modality

When we look at the results for the moderate wind speed modality we can notice a big difference whether it is the winter season or the summer season. In the winter season (Figure 12) almost all turbines (36 of them) present **wind speed** as the variable with the strongest causal effect, whereas 2 of them **relative humidity**. The detailed interactive pie charts Figure 13 show similar beta values throughout all turbines. It is noticeable that even though relative humidity is not the dominant variable for most of the turbines it still has a pretty high beta value in all of them.

5.6 Scenario 6: Summer Half-Year, Moderate Wind Speed Modality

In the summer half-year, the moderate wind scenario seems a bit different than that of the winter half-year. In this seasonal scenario, relative humidity is calculated in each turbine as the most influential variable (Figure 14). In the detailed view of the pie charts in the wind farm in Figure 15 we can see that the causal influence of relative humidity comes with a very high beta value in all of the turbines, higher than in all other scenarios. We can also notice that in the moderate wind scenario, geopotential does not have a big causal influence on wind speed.

Winter half-year, high speed wind

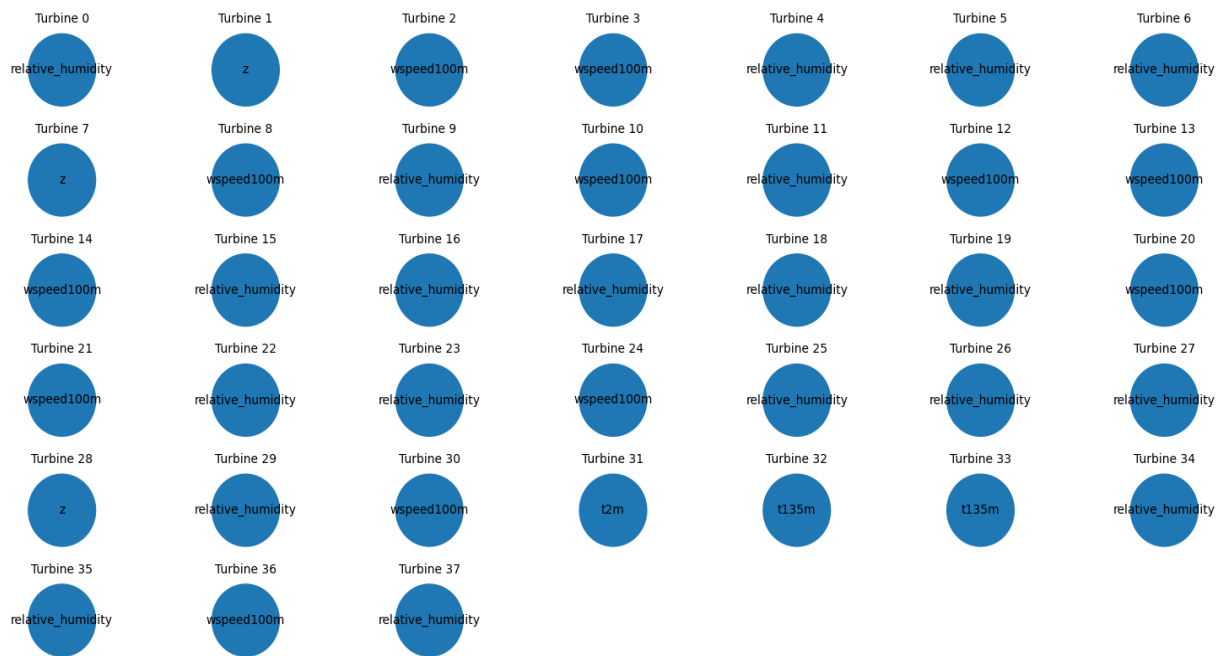


Figure 4: Strongest influential variable on wind speed, Scenario 1

Winter half-year, high speed wind

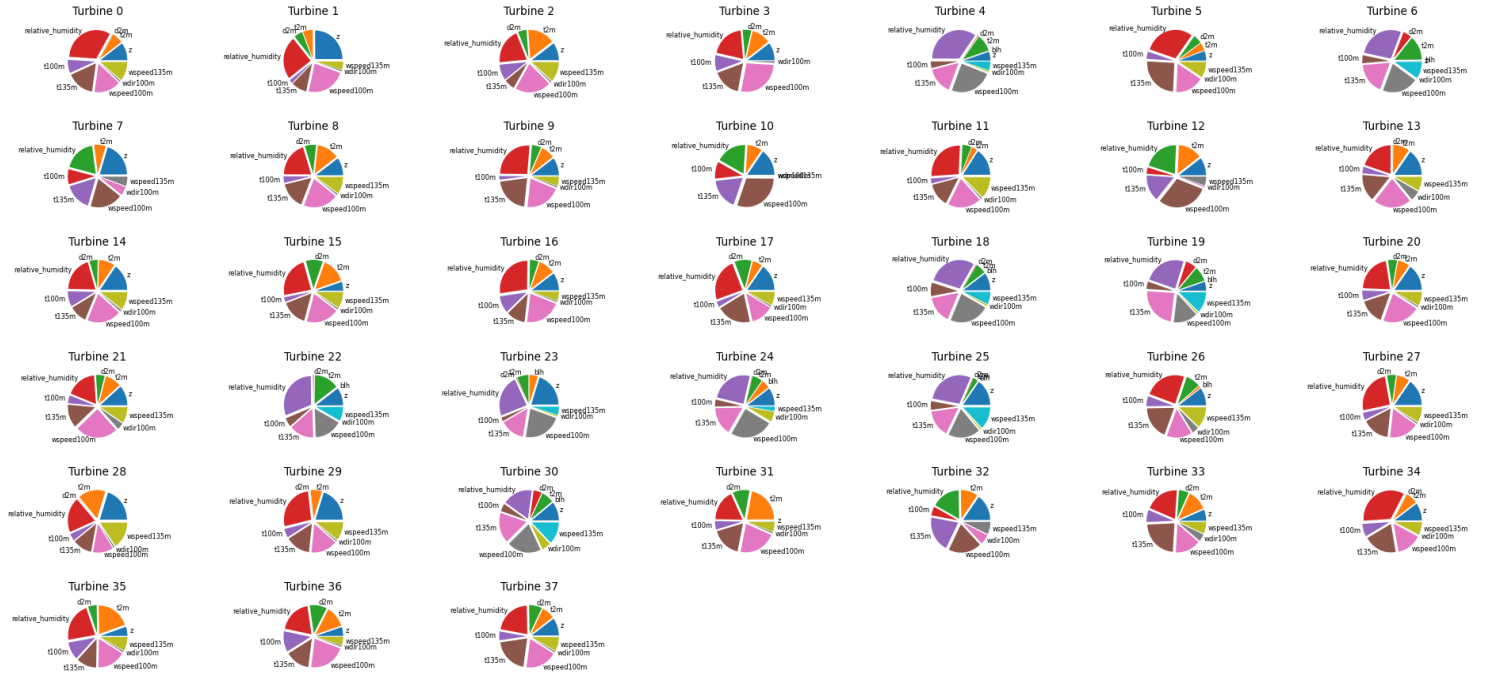


Figure 5: All influential variable on wind speed, Scenario 1

Summer half-year, high speed wind

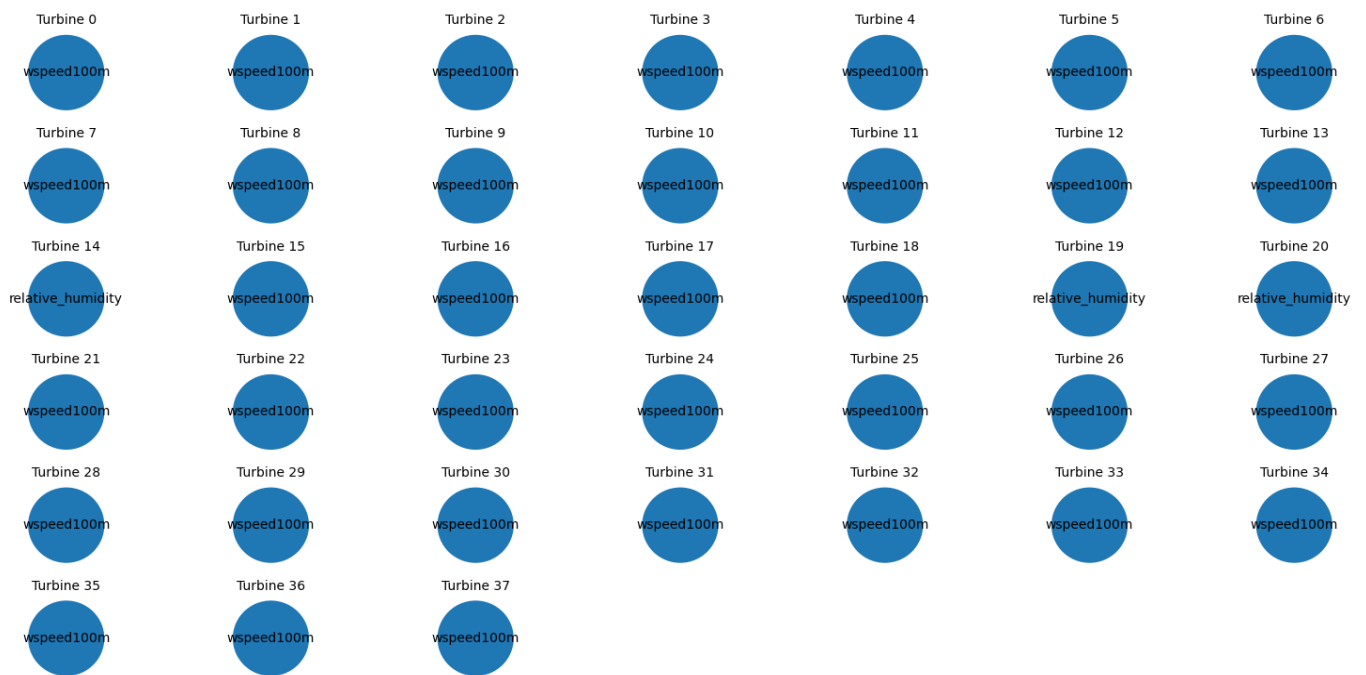


Figure 6: Strongest influential variable on wind speed, Scenario 2

Summer half-year, high speed wind

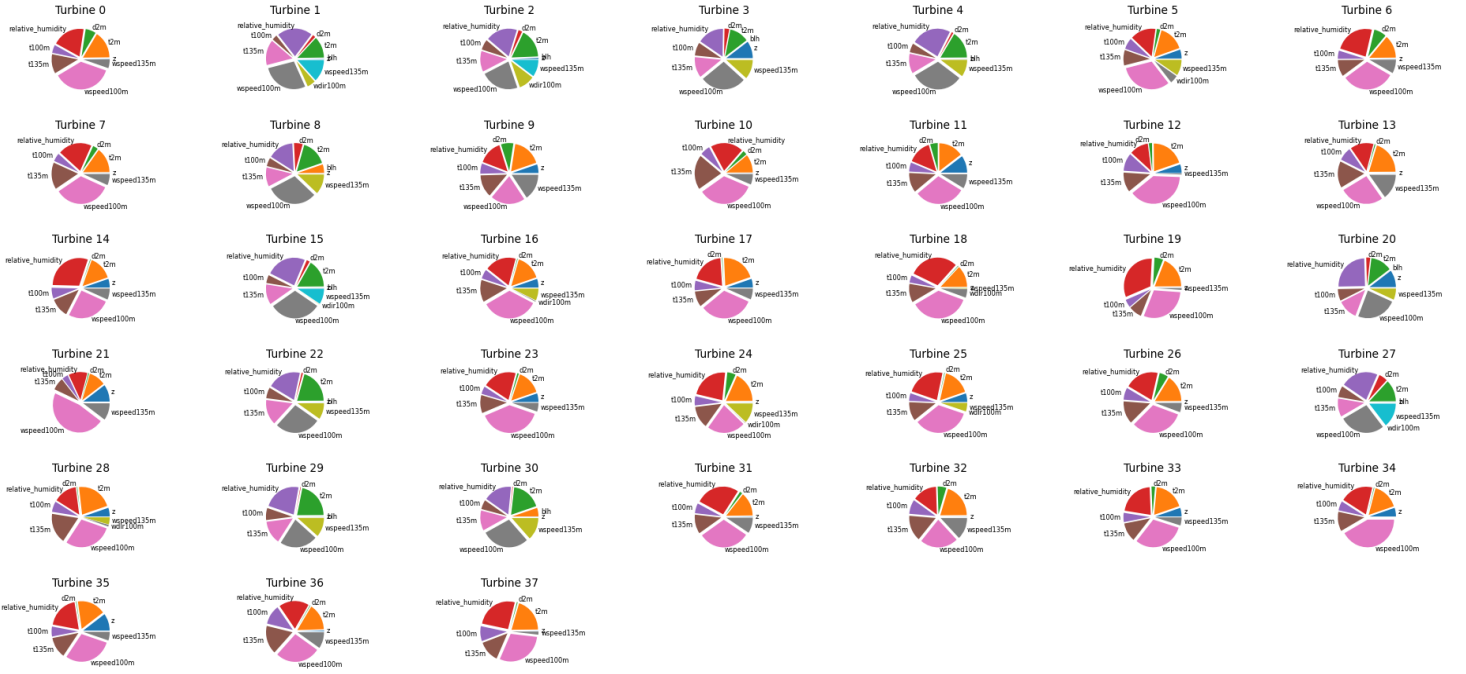


Figure 7: All influential variable on wind speed, Scenario 2

Winter half-year, low speed wind

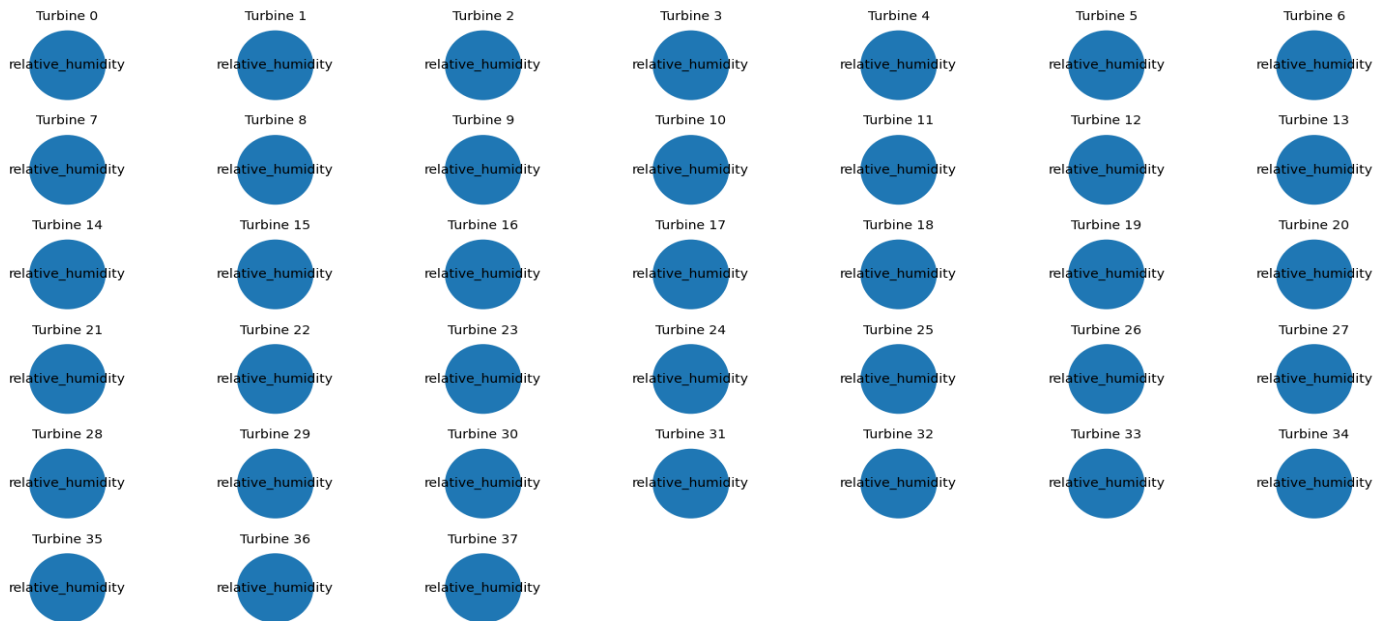


Figure 8: Strongest influential variable on wind speed, Scenario 3

Winter half-year, low speed wind



Figure 9: All influential variables on wind speed, Scenario 3

Summer half-year, low speed wind

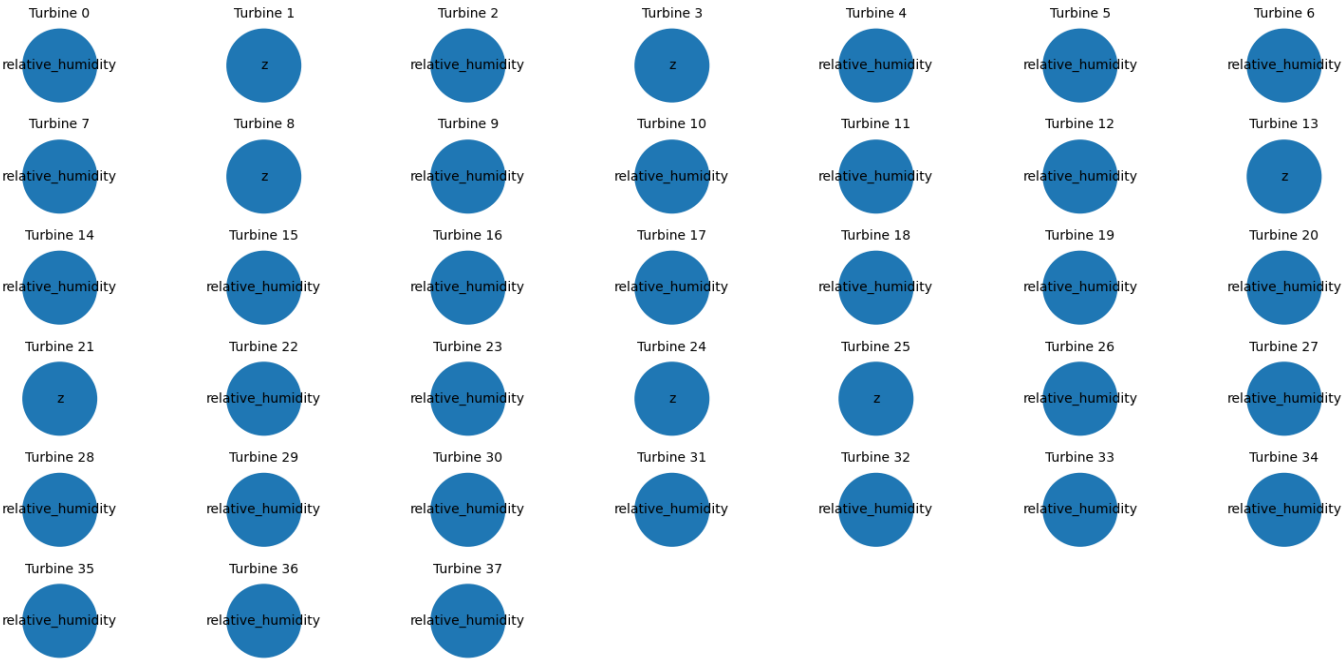


Figure 10: Strongest influential variable on wind speed, Scenario 4

Summer half-year, low speed wind

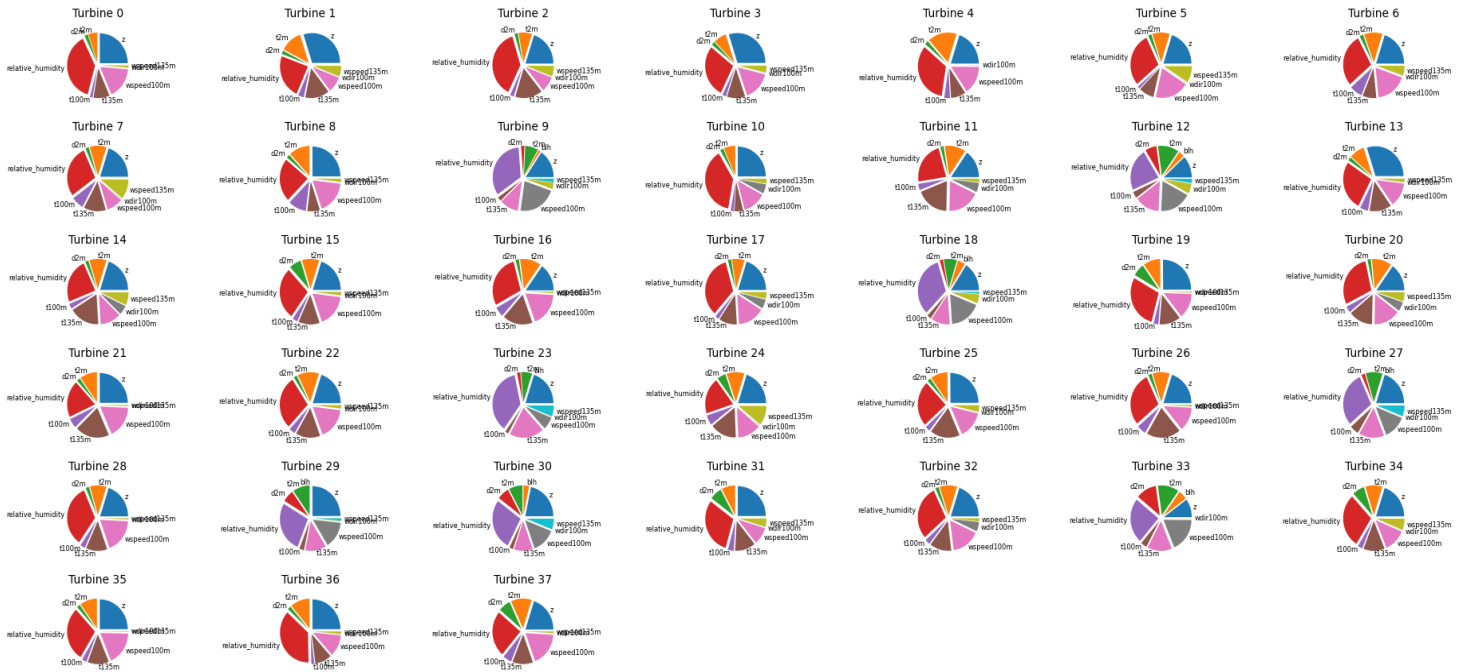


Figure 11: All influential variables on wind speed, Scenario 4

Winter half-year, medium speed wind

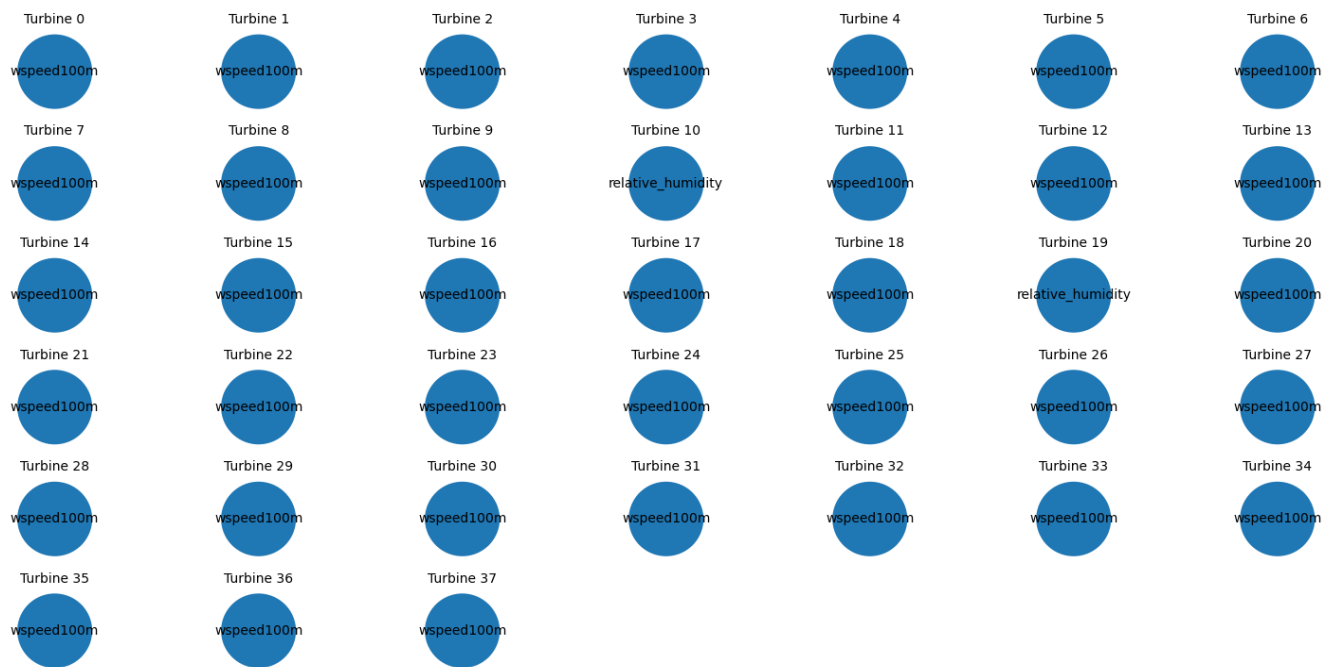


Figure 12: Strongest influential variable on wind speed, Scenario 5

Winter half-year, medium speed wind

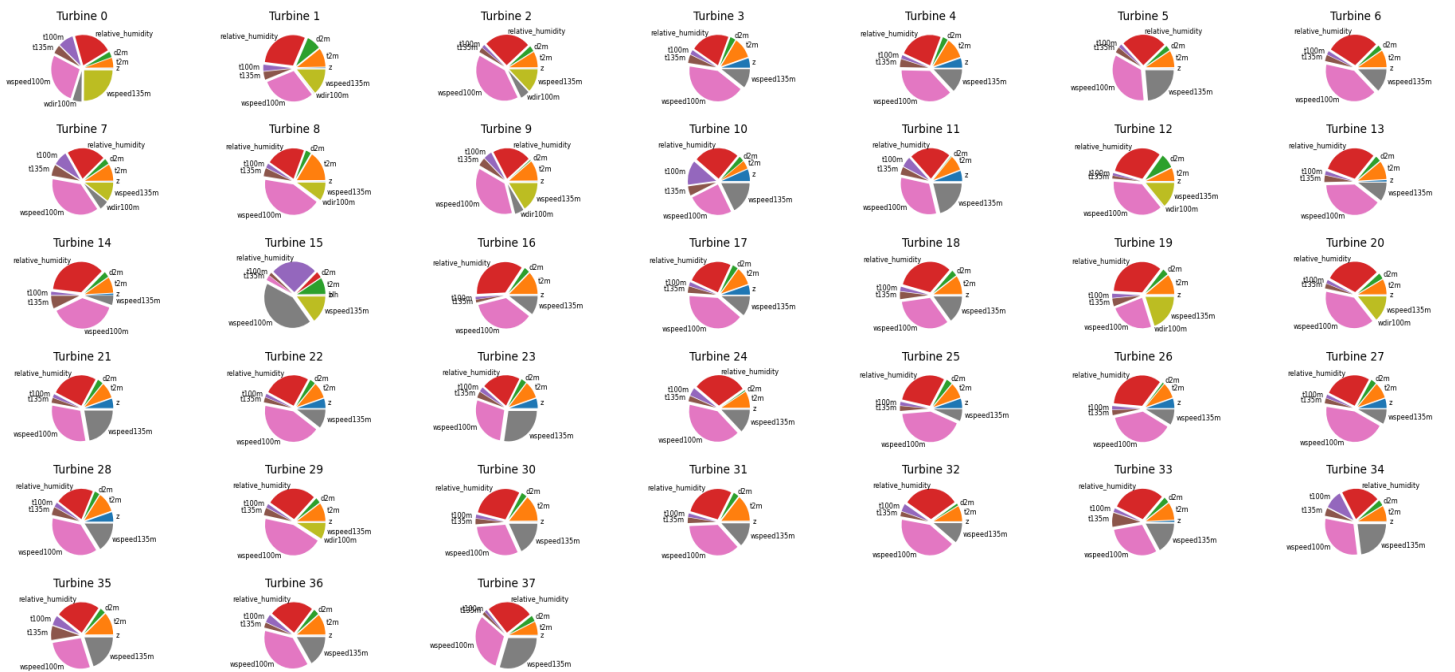


Figure 13: All influential variables on wind speed, Scenario 5

Summer half-year, medium speed wind



Figure 14: Strongest influential variable on wind speed, Scenario 6

Summer half-year, medium speed wind

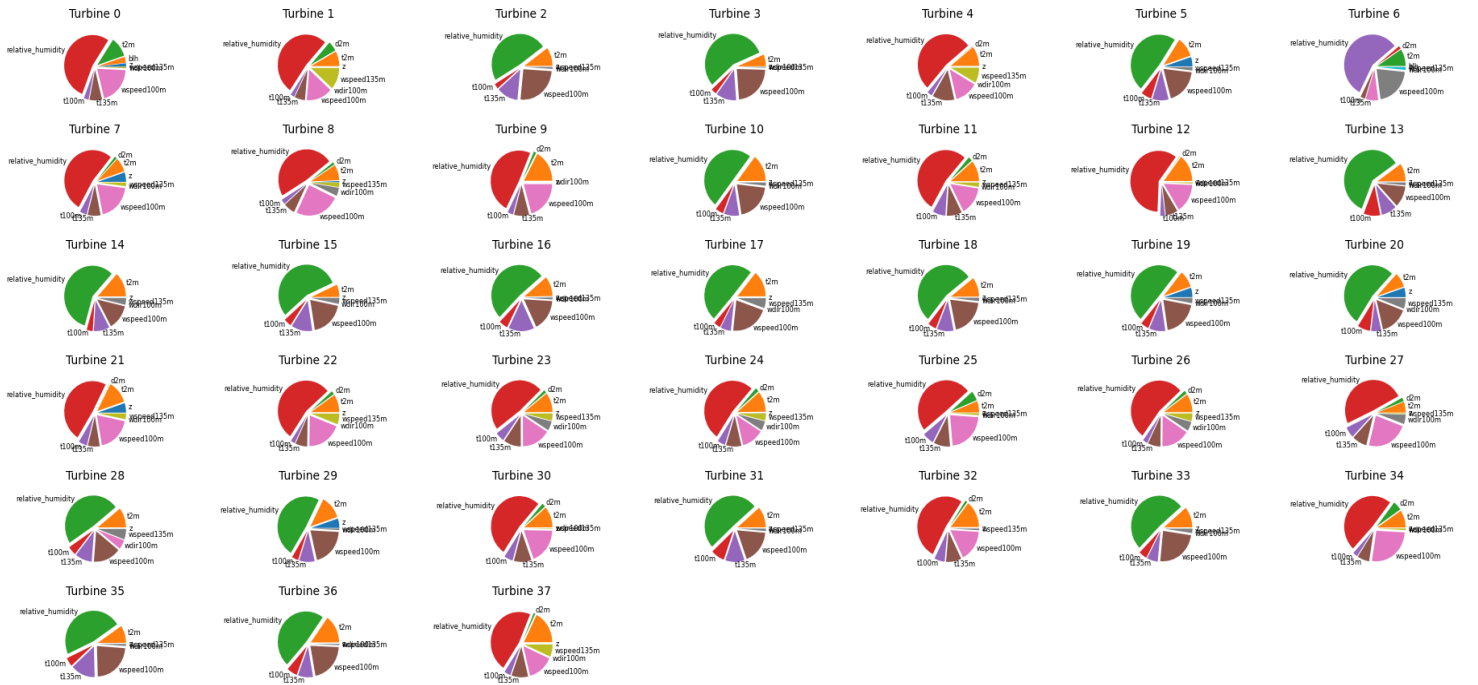


Figure 15: All influential variables on wind speed, Scenario 6

5.7 Beta values

In this section we will go through the specific beta proportionality values which quantify the causal strength in each of the scenarios and each of the turbines in the farm. Each table represents a different scenario, and in each table the variable with the biggest beta value is denoted in bold. The values in each row sum up to 1.

Table 3: Beta values for scenario winter half-year, high wind speed

Variables										
Turbines	bhl	d2m	z	r	t2m	t100m	t135m	wdir100m	wspeed135m	wspeed100m
T0	0.000	0.000	0.050	0.280	0.137	0.071	0.168	0.009	0.103	0.182
T1	0.000	0.051	0.151	0.293	0.046	0.036	0.151	0.008	0.047	0.217
T2	0.000	0.051	0.151	0.215	0.204	0.024	0.122	0.000	0.078	0.156
T3	0.000	0.101	0.102	0.245	0.096	0.040	0.155	0.009	0.047	0.206
T4	0.000	0.004	0.050	0.349	0.047	0.088	0.153	0.008	0.054	0.247
T5	0.000	0.051	0.053	0.334	0.076	0.043	0.220	0.000	0.110	0.112
T6	0.000	0.051	0.102	0.270	0.060	0.054	0.171	0.000	0.129	0.163
T7	0.000	0.001	0.200	0.195	0.093	0.020	0.130	0.057	0.113	0.191
T8	0.000	0.067	0.150	0.201	0.082	0.037	0.153	0.008	0.067	0.236
T9	0.000	0.059	0.151	0.222	0.087	0.094	0.125	0.000	0.052	0.209
T10	0.000	0.002	0.251	0.209	0.067	0.061	0.108	0.008	0.111	0.183
T11	0.000	0.004	0.207	0.294	0.077	0.091	0.114	0.000	0.091	0.122
T12	0.000	0.000	0.101	0.225	0.125	0.090	0.174	0.008	0.110	0.167
T13	0.000	0.001	0.151	0.219	0.110	0.104	0.121	0.050	0.050	0.194
T14	0.000	0.048	0.152	0.200	0.096	0.037	0.152	0.010	0.094	0.210
T15	0.000	0.151	0.050	0.201	0.097	0.037	0.152	0.008	0.053	0.251
T16	0.000	0.052	0.101	0.254	0.157	0.050	0.120	0.008	0.063	0.194
T17	0.000	0.153	0.150	0.265	0.048	0.077	0.093	0.008	0.072	0.134
T18	0.000	0.012	0.100	0.326	0.046	0.039	0.202	0.009	0.100	0.166
T19	0.000	0.064	0.051	0.198	0.082	0.042	0.243	0.008	0.159	0.154
T20	0.000	0.053	0.050	0.219	0.122	0.079	0.170	0.008	0.150	0.149
T21	0.000	0.053	0.065	0.265	0.123	0.040	0.123	0.038	0.117	0.176
T22	0.000	0.003	0.150	0.279	0.084	0.056	0.134	0.008	0.053	0.234
T23	0.050	0.003	0.201	0.285	0.078	0.020	0.145	0.000	0.054	0.163
T24	0.050	0.004	0.051	0.404	0.065	0.022	0.140	0.100	0.077	0.087
T25	0.001	0.001	0.150	0.290	0.047	0.036	0.151	0.008	0.127	0.190
T26	0.010	0.001	0.103	0.271	0.091	0.050	0.165	0.040	0.147	0.122
T27	0.000	0.001	0.201	0.190	0.126	0.037	0.165	0.008	0.115	0.157
T28	0.000	0.001	0.151	0.273	0.190	0.037	0.179	0.000	0.060	0.109
T29	0.000	0.010	0.201	0.248	0.078	0.029	0.104	0.007	0.090	0.233
T30	0.000	0.049	0.157	0.167	0.072	0.024	0.151	0.053	0.215	0.111
T31	0.000	0.102	0.001	0.239	0.195	0.038	0.155	0.008	0.199	0.065
T32	0.001	0.001	0.201	0.199	0.088	0.067	0.121	0.056	0.103	0.163
T33	0.000	0.011	0.101	0.199	0.087	0.091	0.242	0.008	0.119	0.142
T34	0.000	0.000	0.051	0.262	0.188	0.043	0.226	0.000	0.100	0.129

T35	0.000	0.050	0.052	0.179	0.227	0.045	0.175	0.008	0.069	0.195
T36	0.000	0.053	0.101	0.278	0.094	0.079	0.143	0.008	0.062	0.182
T37	0.000	0.028	0.101	0.240	0.118	0.022	0.168	0.008	0.071	0.244

Table 4: Beta values for scenario summer half-year, high wind speed

Variables										
Turbines	bhl	d2m	z	r	t2m	t100m	t135m	wdir100m	wspeed135m	wspeed100m
T0	0.000	0.053	0.001	0.194	0.160	0.046	0.113	0.000	0.205	0.227
T1	0.000	0.016	0.101	0.151	0.154	0.044	0.111	0.000	0.110	0.313
T2	0.000	0.023	0.006	0.239	0.148	0.051	0.113	0.095	0.065	0.260
T3	0.000	0.029	0.101	0.152	0.162	0.069	0.135	0.000	0.110	0.241
T4	0.000	0.003	0.001	0.333	0.183	0.059	0.132	0.000	0.024	0.265
T5	0.000	0.021	0.052	0.126	0.144	0.064	0.084	0.048	0.130	0.331
T6	0.000	0.023	0.001	0.149	0.193	0.064	0.168	0.000	0.082	0.321
T7	0.000	0.081	0.001	0.156	0.148	0.048	0.157	0.000	0.144	0.265
T8	0.050	0.074	0.001	0.232	0.097	0.053	0.088	0.000	0.007	0.398
T9	0.000	0.075	0.050	0.115	0.163	0.058	0.125	0.000	0.061	0.353
T10	0.000	0.025	0.050	0.228	0.129	0.049	0.152	0.000	0.106	0.260
T11	0.037	0.022	0.066	0.143	0.151	0.055	0.117	0.048	0.089	0.273
T12	0.000	0.023	0.050	0.143	0.199	0.053	0.114	0.000	0.180	0.237
T13	0.000	0.006	0.001	0.142	0.201	0.096	0.139	0.000	0.105	0.311
T14	0.000	0.003	0.050	0.353	0.125	0.079	0.123	0.000	0.112	0.155
T15	0.000	0.019	0.001	0.175	0.149	0.067	0.130	0.001	0.184	0.274
T16	0.000	0.003	0.050	0.141	0.156	0.056	0.132	0.004	0.172	0.286
T17	0.000	0.003	0.050	0.240	0.160	0.057	0.095	0.000	0.132	0.262
T18	0.000	0.003	0.001	0.318	0.099	0.049	0.072	0.050	0.061	0.347
T19	0.000	0.053	0.001	0.212	0.144	0.027	0.055	0.000	0.008	0.500
T20	0.000	0.022	0.101	0.219	0.133	0.081	0.137	0.000	0.067	0.241
T21	0.000	0.005	0.101	0.234	0.139	0.047	0.102	0.000	0.059	0.314
T22	0.000	0.009	0.001	0.212	0.161	0.066	0.179	0.000	0.094	0.277
T23	0.000	0.005	0.050	0.278	0.135	0.042	0.098	0.000	0.050	0.342
T24	0.000	0.051	0.001	0.266	0.156	0.046	0.112	0.002	0.020	0.346
T25	0.000	0.003	0.050	0.234	0.142	0.039	0.094	0.000	0.078	0.361
T26	0.000	0.052	0.001	0.240	0.162	0.052	0.118	0.000	0.156	0.218
T27	0.000	0.060	0.001	0.226	0.150	0.072	0.125	0.000	0.085	0.281
T28	0.000	0.003	0.051	0.113	0.200	0.062	0.163	0.010	0.000	0.397
T29	0.000	0.003	0.001	0.141	0.202	0.071	0.132	0.000	0.122	0.329
T30	0.000	0.003	0.001	0.198	0.189	0.051	0.117	0.000	0.111	0.329
T31	0.000	0.049	0.002	0.198	0.194	0.053	0.126	0.000	0.135	0.243
T32	0.000	0.053	0.001	0.113	0.217	0.058	0.135	0.000	0.156	0.267
T33	0.000	0.022	0.101	0.194	0.190	0.040	0.099	0.000	0.011	0.344
T34	0.000	0.003	0.050	0.247	0.135	0.050	0.101	0.000	0.005	0.409
T35	0.000	0.003	0.101	0.226	0.126	0.077	0.129	0.000	0.066	0.272
T36	0.000	0.003	0.005	0.217	0.148	0.090	0.240	0.000	0.010	0.287
T37	0.000	0.003	0.002	0.201	0.161	0.099	0.119	0.000	0.059	0.356

Table 5: Beta values for scenario winter half-year, low wind speed

Variables										
Turbines	bhl	d2m	z	r	t2m	t100m	t135m	wdir100m	wspeed135m	wspeed100m
T0	0.000	0.020	0.050	0.458	0.077	0.055	0.050	0.000	0.140	0.150
T1	0.000	0.014	0.101	0.315	0.089	0.053	0.056	0.050	0.044	0.278
T2	0.000	0.015	0.101	0.358	0.107	0.057	0.066	0.000	0.028	0.268
T3	0.000	0.015	0.051	0.375	0.148	0.068	0.048	0.000	0.038	0.258
T4	0.000	0.015	0.150	0.360	0.104	0.056	0.064	0.000	0.032	0.219
T5	0.000	0.107	0.058	0.319	0.066	0.093	0.080	0.000	0.091	0.186
T6	0.045	0.058	0.056	0.335	0.134	0.044	0.105	0.000	0.059	0.165
T7	0.000	0.062	0.001	0.333	0.125	0.059	0.093	0.000	0.031	0.295
T8	0.000	0.012	0.050	0.295	0.105	0.081	0.130	0.001	0.085	0.241
T9	0.000	0.015	0.061	0.329	0.160	0.083	0.059	0.000	0.012	0.281
T10	0.000	0.105	0.061	0.338	0.082	0.038	0.095	0.000	0.037	0.244
T11	0.000	0.049	0.050	0.401	0.089	0.053	0.130	0.000	0.157	0.069
T12	0.000	0.044	0.099	0.276	0.102	0.106	0.000	0.000	0.159	0.215
T13	0.000	0.018	0.050	0.409	0.139	0.079	0.080	0.000	0.038	0.187
T14	0.000	0.051	0.109	0.382	0.083	0.055	0.059	0.000	0.099	0.162
T15	0.000	0.015	0.050	0.350	0.080	0.104	0.102	0.000	0.068	0.231
T16	0.000	0.020	0.050	0.425	0.114	0.092	0.092	0.000	0.035	0.171
T17	0.000	0.010	0.101	0.428	0.131	0.066	0.042	0.000	0.060	0.162
T18	0.000	0.018	0.160	0.323	0.078	0.064	0.075	0.000	0.052	0.230
T19	0.000	0.006	0.061	0.366	0.183	0.056	0.064	0.000	0.054	0.211
T20	0.000	0.015	0.150	0.325	0.092	0.036	0.075	0.050	0.039	0.217
T21	0.000	0.015	0.101	0.360	0.128	0.083	0.066	0.000	0.028	0.218
T22	0.000	0.018	0.101	0.363	0.096	0.105	0.060	0.000	0.088	0.169
T23	0.045	0.018	0.056	0.305	0.102	0.069	0.100	0.050	0.028	0.228
T24	0.000	0.007	0.151	0.376	0.063	0.041	0.069	0.000	0.047	0.246
T25	0.000	0.023	0.027	0.444	0.131	0.059	0.052	0.024	0.066	0.175
T26	0.000	0.021	0.101	0.465	0.118	0.028	0.054	0.000	0.081	0.133
T27	0.000	0.021	0.151	0.426	0.067	0.041	0.042	0.049	0.044	0.160
T28	0.000	0.068	0.050	0.382	0.091	0.053	0.053	0.050	0.082	0.170
T29	0.000	0.019	0.150	0.430	0.045	0.041	0.065	0.000	0.000	0.251
T30	0.000	0.115	0.109	0.364	0.069	0.029	0.098	0.000	0.011	0.204
T31	0.000	0.059	0.050	0.402	0.105	0.027	0.052	0.000	0.050	0.255
T32	0.000	0.018	0.210	0.322	0.066	0.037	0.104	0.000	0.069	0.174
T33	0.000	0.008	0.101	0.330	0.162	0.029	0.056	0.050	0.102	0.163
T34	0.000	0.008	0.101	0.368	0.110	0.031	0.113	0.005	0.117	0.147
T35	0.045	0.067	0.106	0.288	0.118	0.041	0.043	0.000	0.079	0.214
T36	0.000	0.067	0.101	0.343	0.116	0.028	0.053	0.000	0.034	0.258
T37	0.000	0.015	0.115	0.413	0.106	0.035	0.058	0.000	0.041	0.216

Table 6: Beta values for scenario summer half-year, low wind speed

Variables										
Turbines	bhl	d2m	z	r	t2m	t100m	t135m	wdir100m	wspeed135m	wspeed100m
T0	0.000	0.019	0.250	0.423	0.060	0.016	0.096	0.001	0.015	0.121
T1	0.000	0.019	0.300	0.272	0.115	0.029	0.130	0.001	0.000	0.134
T2	0.000	0.019	0.200	0.411	0.067	0.019	0.150	0.001	0.012	0.120
T3	0.000	0.019	0.250	0.356	0.068	0.018	0.100	0.001	0.008	0.180
T4	0.000	0.021	0.201	0.418	0.080	0.022	0.108	0.001	0.000	0.149
T5	0.050	0.069	0.101	0.276	0.139	0.040	0.131	0.001	0.000	0.193
T6	0.000	0.021	0.200	0.327	0.106	0.025	0.132	0.001	0.009	0.179
T7	0.000	0.018	0.190	0.358	0.100	0.038	0.105	0.001	0.011	0.180
T8	0.000	0.019	0.200	0.275	0.149	0.050	0.108	0.001	0.012	0.184
T9	0.012	0.020	0.204	0.289	0.071	0.020	0.103	0.034	0.029	0.217
T10	0.000	0.020	0.201	0.394	0.064	0.027	0.089	0.051	0.017	0.138
T11	0.000	0.020	0.202	0.235	0.121	0.034	0.186	0.001	0.058	0.143
T12	0.000	0.068	0.174	0.328	0.079	0.025	0.113	0.004	0.069	0.141
T13	0.000	0.069	0.300	0.282	0.073	0.021	0.104	0.001	0.029	0.120
T14	0.000	0.020	0.150	0.291	0.099	0.028	0.123	0.101	0.029	0.160
T15	0.000	0.019	0.250	0.323	0.079	0.023	0.110	0.001	0.057	0.138
T16	0.000	0.019	0.150	0.289	0.122	0.054	0.174	0.001	0.067	0.124
T17	0.000	0.019	0.250	0.342	0.073	0.021	0.104	0.001	0.014	0.176
T18	0.000	0.019	0.250	0.241	0.122	0.035	0.141	0.001	0.007	0.184
T19	0.000	0.068	0.251	0.257	0.093	0.026	0.118	0.001	0.003	0.183
T20	0.000	0.019	0.150	0.327	0.103	0.029	0.129	0.051	0.007	0.184
T21	0.000	0.019	0.250	0.259	0.092	0.051	0.193	0.001	0.014	0.120
T22	0.000	0.069	0.200	0.288	0.100	0.028	0.123	0.001	0.020	0.171
T23	0.000	0.019	0.201	0.332	0.077	0.024	0.212	0.001	0.057	0.078
T24	0.000	0.069	0.250	0.287	0.074	0.045	0.129	0.001	0.010	0.134
T25	0.000	0.019	0.251	0.297	0.074	0.021	0.154	0.001	0.006	0.177
T26	0.000	0.019	0.201	0.343	0.053	0.040	0.163	0.001	0.063	0.117
T27	0.000	0.069	0.151	0.347	0.050	0.039	0.113	0.001	0.072	0.157
T28	0.000	0.019	0.201	0.288	0.099	0.027	0.122	0.050	0.000	0.195
T29	0.012	0.066	0.200	0.258	0.105	0.027	0.124	0.042	0.016	0.149
T30	0.032	0.069	0.217	0.286	0.073	0.021	0.104	0.001	0.000	0.196
T31	0.021	0.069	0.229	0.266	0.099	0.040	0.133	0.001	0.000	0.142
T32	0.000	0.019	0.250	0.302	0.118	0.033	0.137	0.001	0.018	0.122
T33	0.000	0.119	0.150	0.291	0.149	0.028	0.123	0.001	0.016	0.124
T34	0.000	0.069	0.200	0.243	0.150	0.028	0.123	0.001	0.021	0.165
T35	0.000	0.019	0.250	0.295	0.149	0.028	0.073	0.001	0.009	0.177
T36	0.000	0.011	0.251	0.241	0.149	0.028	0.123	0.002	0.007	0.189
T37	0.000	0.120	0.150	0.241	0.125	0.052	0.123	0.001	0.029	0.159

Table 7: Beta values for scenario winter half-year, moderate wind speed

Variables										
Turbines	bhl	d2m	z	r	t2m	t100m	t135m	wdir100m	wspeed135m	wspeed100m
T0	0.000	0.029	0.001	0.214	0.102	0.035	0.046	0.050	0.146	0.377
T1	0.000	0.029	0.003	0.345	0.085	0.029	0.032	0.001	0.078	0.397
T2	0.000	0.030	0.001	0.262	0.085	0.018	0.027	0.050	0.099	0.428
T3	0.000	0.002	0.050	0.271	0.102	0.046	0.042	0.000	0.084	0.402
T4	0.000	0.029	0.009	0.269	0.084	0.017	0.068	0.000	0.100	0.425
T5	0.000	0.028	0.001	0.257	0.088	0.019	0.029	0.000	0.104	0.473
T6	0.000	0.002	0.001	0.295	0.112	0.020	0.033	0.000	0.061	0.476
T7	0.000	0.028	0.001	0.200	0.144	0.031	0.067	0.050	0.220	0.260
T8	0.000	0.031	0.001	0.314	0.150	0.021	0.034	0.000	0.238	0.210
T9	0.000	0.030	0.001	0.217	0.103	0.020	0.039	0.050	0.222	0.317
T10	0.000	0.028	0.057	0.215	0.107	0.039	0.059	0.000	0.124	0.371
T11	0.000	0.029	0.052	0.296	0.068	0.020	0.022	0.000	0.157	0.355
T12	0.000	0.077	0.001	0.311	0.068	0.012	0.015	0.001	0.179	0.335
T13	0.000	0.030	0.008	0.353	0.085	0.017	0.027	0.000	0.127	0.353
T14	0.000	0.030	0.001	0.315	0.107	0.025	0.045	0.000	0.167	0.310
T15	0.000	0.030	0.001	0.216	0.108	0.025	0.045	0.000	0.124	0.451
T16	0.000	0.030	0.001	0.217	0.107	0.025	0.044	0.050	0.150	0.375
T17	0.000	0.030	0.001	0.266	0.108	0.026	0.045	0.000	0.072	0.452
T18	0.000	0.005	0.007	0.327	0.100	0.089	0.040	0.000	0.225	0.208
T19	0.000	0.036	0.001	0.312	0.100	0.027	0.043	0.000	0.149	0.331
T20	0.000	0.030	0.001	0.268	0.082	0.019	0.027	0.000	0.140	0.434
T21	0.000	0.005	0.008	0.353	0.072	0.037	0.059	0.000	0.085	0.381
T22	0.000	0.030	0.050	0.260	0.080	0.013	0.022	0.000	0.153	0.391
T23	0.000	0.030	0.001	0.258	0.037	0.071	0.029	0.050	0.130	0.393
T24	0.000	0.028	0.001	0.258	0.083	0.021	0.028	0.000	0.150	0.431
T25	0.000	0.033	0.050	0.299	0.084	0.019	0.027	0.000	0.087	0.400
T26	0.000	0.006	0.050	0.301	0.103	0.019	0.026	0.000	0.224	0.271
T27	0.000	0.030	0.050	0.264	0.085	0.018	0.027	0.000	0.058	0.468
T28	0.000	0.028	0.050	0.247	0.092	0.021	0.033	0.000	0.179	0.349
T29	0.000	0.028	0.001	0.272	0.085	0.035	0.046	0.000	0.206	0.326
T30	0.000	0.030	0.050	0.294	0.038	0.019	0.080	0.000	0.150	0.338
T31	0.000	0.029	0.001	0.255	0.137	0.019	0.028	0.000	0.150	0.380
T32	0.000	0.030	0.001	0.361	0.036	0.019	0.027	0.000	0.071	0.454
T33	0.000	0.028	0.001	0.327	0.085	0.018	0.027	0.000	0.231	0.284
T34	0.000	0.030	0.000	0.260	0.119	0.045	0.043	0.000	0.077	0.427
T35	0.000	0.029	0.008	0.290	0.116	0.048	0.114	0.000	0.079	0.317
T36	0.000	0.031	0.001	0.262	0.110	0.043	0.027	0.000	0.156	0.370
T37	0.000	0.028	0.001	0.252	0.073	0.014	0.018	0.000	0.298	0.315

Table 8: Beta values for scenario summer half-year, moderate wind speed

Variables										
Turbines	bhl	d2m	z	r	t2m	t100m	t135m	wdir100m	wspeed135m	wspeed100m
T0	0.031	0.000	0.019	0.493	0.126	0.045	0.076	0.000	0.016	0.194
T1	0.000	0.050	0.001	0.471	0.120	0.035	0.083	0.000	0.072	0.168
T2	0.000	0.000	0.000	0.527	0.079	0.022	0.108	0.000	0.125	0.140
T3	0.000	0.000	0.000	0.515	0.093	0.026	0.118	0.000	0.021	0.227
T4	0.000	0.000	0.000	0.471	0.115	0.048	0.149	0.000	0.010	0.207
T5	0.000	0.021	0.050	0.520	0.088	0.042	0.080	0.000	0.005	0.194
T6	0.000	0.015	0.000	0.533	0.104	0.035	0.084	0.000	0.003	0.226
T7	0.000	0.013	0.050	0.528	0.095	0.027	0.069	0.000	0.009	0.208
T8	0.000	0.013	0.000	0.484	0.097	0.027	0.121	0.000	0.055	0.203
T9	0.000	0.012	0.000	0.484	0.151	0.047	0.093	0.000	0.054	0.159
T10	0.000	0.000	0.000	0.501	0.146	0.043	0.087	0.000	0.020	0.203
T11	0.000	0.009	0.000	0.563	0.114	0.074	0.088	0.000	0.019	0.133
T12	0.000	0.000	0.000	0.579	0.147	0.045	0.087	0.000	0.061	0.082
T13	0.000	0.000	0.000	0.637	0.129	0.040	0.075	0.000	0.055	0.064
T14	0.000	0.000	0.000	0.574	0.119	0.037	0.079	0.000	0.056	0.135
T15	0.000	0.000	0.000	0.546	0.091	0.050	0.139	0.000	0.036	0.138
T16	0.000	0.000	0.003	0.490	0.113	0.033	0.133	0.000	0.069	0.159
T17	0.000	0.000	0.000	0.485	0.169	0.037	0.092	0.000	0.016	0.201
T18	0.000	0.000	0.000	0.535	0.101	0.048	0.093	0.000	0.053	0.170
T19	0.000	0.017	0.050	0.440	0.119	0.059	0.111	0.000	0.011	0.193
T20	0.000	0.000	0.101	0.444	0.090	0.047	0.088	0.000	0.065	0.165
T21	0.000	0.049	0.051	0.483	0.077	0.040	0.084	0.000	0.008	0.208
T22	0.000	0.015	0.000	0.562	0.079	0.033	0.067	0.000	0.004	0.239
T23	0.000	0.016	0.000	0.477	0.106	0.051	0.100	0.050	0.029	0.170
T24	0.000	0.021	0.001	0.482	0.091	0.060	0.095	0.050	0.007	0.193
T25	0.000	0.000	0.000	0.516	0.078	0.056	0.100	0.050	0.004	0.196
T26	0.000	0.017	0.000	0.564	0.064	0.033	0.065	0.050	0.001	0.206
T27	0.000	0.020	0.000	0.485	0.099	0.028	0.073	0.050	0.000	0.245
T28	0.000	0.000	0.000	0.487	0.106	0.048	0.097	0.050	0.016	0.196
T29	0.000	0.000	0.050	0.486	0.115	0.034	0.080	0.000	0.000	0.235
T30	0.000	0.020	0.000	0.485	0.107	0.089	0.103	0.000	0.080	0.116
T31	0.000	0.000	0.000	0.473	0.139	0.087	0.100	0.000	0.027	0.175
T32	0.000	0.012	0.000	0.543	0.103	0.065	0.113	0.000	0.006	0.159
T33	0.000	0.004	0.000	0.490	0.142	0.055	0.083	0.000	0.095	0.131
T34	0.000	0.050	0.000	0.519	0.059	0.038	0.065	0.000	0.068	0.201
T35	0.000	0.000	0.000	0.510	0.077	0.044	0.127	0.001	0.015	0.226
T36	0.000	0.002	0.000	0.478	0.140	0.048	0.104	0.000	0.019	0.210
T37	0.000	0.011	0.000	0.507	0.167	0.038	0.092	0.000	0.007	0.177

6 Conclusions

As can be seen from results in Section 5 the variables with the strongest causal influence over all scenarios on wind speed are **relative humidity** and **wind speed**. Relative humidity is the one with the highest beta value in scenario summer half-year, moderate wind speed and winter half-year, low wind speed in all turbines (see Table 5,8) in scenario summer half-year, low wind speed it has the highest beta value in 31 turbines (see Table 6).

Wind speed is the most influential in scenarios summer half-year, high wind (Table 4), winter half-year, moderate wind (Table 7) and it shows a big beta value in all of the turbines in scenario winter half-year high wind (Table 4).

As a possible interpretation one can see a difference when looking at the extreme wind modality in comparison with 'calm' periods. For the extreme scenario 'high wind' (Table 3,4) based on the beta values we can see that for both summer and winter half-years wind speed variable is very dominant with the highest beta value in the farm 0.5 measured by Turbine 19 in the summer season. For the extreme scenario 'low wind' (Table 5,6) we can see that relative humidity has the highest beta values across all turbines (to compare with the high wind modality scenario, the highest beta value for wind speed across all farm is 0.217 in the summer season). In both cases the seasonal scenario doesn't seem to have too much of an influence. When observing the periods of moderate wind, the partition between summer and winter half-year is substantive. In moderate wind summer season wind has the highest beta value of 0.245 and in the winter half-year it has the highest value of 0.476 which also makes it the most influential variable for the winter half-year moderate wind modality.

These observations and the descriptions of beta values in the tables in Section 5 conclude the answers for our second and third research questions about the strength of the causal relation of all 10 meteorological variables to wind speed and their differences across the scenarios. The first question is addressed in Section 4 where we explain the implementation in python and for the forth research question about the visualization we can refer to Section 5 where figures of each scenario are shown as well as in Section 4 where an

example from pie charts is mentioned.

7 Future Work

For a possible future work, the sample size of the experiments can be extended. For example a sliding window containing four 96h intervals with one hour difference can be considered instead of one 96h interval for each scenario and each turbine. That would give a even more complete view on how wind/its causal variables behave/change around the time of extremes.

Another future direction can be selecting the scenarios not through prior knowledge but through some automation or clustering by deep learning techniques.

Another work could be also done in visualization. One could for example for one turbine visualize, how the beta values of other 10 variables change in time when we observe a longer time period including several out of our scenarios and this without averaging, only on a concrete data set.

References

- [1] The European centre for medium-range weather forecasts. <https://www.ecmwf.int/en/forecasts>.
- [2] Hydrological half-year. <https://encyclopedia2.thefreedictionary.com/Hydrologic+Year>.
- [3] BAHADORI, M. T., AND LIU, Y. Granger causality analysis in irregular time series. In *SDM* (2012).
- [4] BARTHELMIE, R. J., AND PALUTIKOF, J. P. Coastal wind speed modelling for wind energy applications. *Journal of Wind Engineering and Industrial Aerodynamics* 62 (1996), 213–236.
- [5] BEHZADI, S., HLAVÁČKOVÁ-SCHINDLER, K., AND PLANT, C. Granger causality for heterogeneous processes. In *Advances in Knowledge Discovery and Data Mining* (Cham, 2019), Q. Yang, Z.-H. Zhou, Z. Gong, M.-L. Zhang, and S.-J. Huang, Eds., Springer International Publishing, pp. 463–475.
- [6] BRAUN, P. A., AND MITTNIK, S. Misspecifications in vector autoregressions and their effects on impulse responses and variance decompositions. *Journal of econometrics* 59, 3 (1993), 319–341.
- [7] CADENAS, E., AND RIVERA, W. Wind speed forecasting in the south coast of oaxaca, mexico. *Renewable energy* 32, 12 (2007), 2116–2128.
- [8] CADENAS, E., AND RIVERA, W. Wind speed forecasting in the south coast of oaxaca, méxico. *Renewable Energy* 32 (10 2007), 2116–2128.
- [9] CADENAS, E., AND RIVERA, W. Wind speed forecasting in three different regions of mexico, using a hybrid arima–ann model. *Renewable Energy* 35, 12 (2010), 2732–2738.
- [10] CAROLIN MABEL, M., AND FERNANDEZ, E. Analysis of wind power generation and prediction using ann: A case study. *Renewable Energy* 33, 5 (2008), 986–992.
- [11] COLQUHOUN, J. R., AND RILEY, P. A. Relationships between tornado intensity and various wind and thermodynamic variables. *Weather and Forecasting* 11, 3 (1996), 360 – 371.
- [12] EICHLER, M. Causal inference with multiple time series: principles and problems. *Philosophical Transactions of the Royal Society A: Mathematical, Physical and Engineering Sciences* 371, 1997 (2013), 20110613.

- [13] FOLEY, A. M., LEAHY, P. G., MARVUGLIA, A., AND MCKEOGH, E. J. Current methods and advances in forecasting of wind power generation. *Renewable Energy* 37 (1 2012), 1–8.
- [14] GOEBEL, R., ROEBROECK, A., KIM, D.-S., AND FORMISANO, E. Investigating directed cortical interactions in time-resolved fmri data using vector autoregressive modeling and granger causality mapping. *Magnetic Resonance Imaging* 21, 10 (2003), 1251–1261.
- [15] GRANGER, C. W. Investigating causal relations by econometric models and cross-spectral methods. *Econometrica: journal of the Econometric Society* (1969), 424–438.
- [16] HLAVÁČKOVÁ-SCHINDLER, K., AND PLANT, C. Heterogeneous graphical granger causality by minimum message length. *Entropy* 2020, Vol. 22, Page 1400 22 (12 2020), 1400.
- [17] LIN, Z., AND LIU, X. Wind power forecasting of an offshore wind turbine based on high-frequency scada data and deep learning neural network. *Energy* 201 (2020), 117693.
- [18] LIU, D., NIU, D., WANG, H., AND FAN, L. Short-term wind speed forecasting using wavelet transform and support vector machines optimized by genetic algorithm. *Renewable Energy* 62 (2014), 592–597.
- [19] MANNINO, M., AND BRESSLER, S. L. Foundational perspectives on causality in large-scale brain networks. *Physics of life reviews* 15 (2015), 107–123.
- [20] MARINESCU, I. E., LAWLOR, P. N., AND KORDING, K. P. Quasi-experimental causality in neuroscience and behavioural research. *Nature Human Behaviour* 2, 12 (December 2018), 891.
- [21] MAZIARZ, M. A review of the granger-causality fallacy. *Journal of Philosophical Economics Volume VIII Issue 2* (05 2015).
- [22] MONFARED, M., RASTEGAR, H., AND KOJABADI, H. M. A new strategy for wind speed forecasting using artificial intelligent methods. *Renewable Energy* 34, 3 (2009), 845–848.
- [23] OZCICEK, O., AND MCMILLIN, W. D. Lag length selection in vector autoregressive models: symmetric and asymmetric lags. *Applied Economics* 31, 4 (1999), 517–524.
- [24] PELLETIER, F., MASSON, C., AND TAHAN, A. Wind turbine power curve modelling using artificial neural network. *Renewable Energy* 89 (2016), 207–214.

- [25] PORTÉ-AGEL, F., BASTANKHAH, M., AND SHAMSODDIN, S. Wind-turbine and wind-farm flows: a review. *Boundary-Layer Meteorology* 174, 1 (2020), 1–59.
- [26] SHI, J., GUO, J., AND ZHENG, S. Evaluation of hybrid forecasting approaches for wind speed and power generation time series. *Renewable and Sustainable Energy Reviews* 16, 5 (2012), 3471–3480.
- [27] SHOJAIE, A., AND MICHAILIDIS, G. Discovering graphical Granger causality using the truncating lasso penalty. *Bioinformatics* 26, 18 (09 2010), i517–i523.
- [28] STUMPO, M., CONSOLINI, G., AND ALBERTI, T. Causal inference in space weather by an information theory approach. *Journal of Physics: Conference Series* 1548, 1 (may 2020), 012019.
- [29] WALLACE, C. S., AND DOWE, D. L. Minimum message length and kolmogorov complexity. *The Computer Journal* 42, 4 (1999), 270–283.
- [30] WALLACE, C. S., AND FREEMAN, P. R. Estimation and inference by compact coding. *Journal of the Royal Statistical Society: Series B (Methodological)* 49, 3 (1987), 240–252.